Men With Brugada-Like Electrocardiogram Have Higher Risk of Prostate Cancer

Daisuke Haruta, MD*,**,‡; Kiyotaka Matsuo, MD*,**,‡; Shinichiro Ichimaru, MS**; Midori Soda, MD†; Ayumi Hida, MD**; Nobuko Sera, MD**; Misa Imaizumi, MD**; Eiji Nakashima, PhD††; Shinji Seto, MD*,**; Masazumi Akahoshi, MD**

Background Elevated plasma testosterone levels are thought to play a role in the male preponderance of cases of Brugada syndrome (BS) and the development of prostate cancer.

Methods and Results The 34 Brugada-like electrocardiogram (ECG) cases were identified among 2,681 male survivors of the atomic bomb who had undergone at least 1 biennial health examination between July 1958 and December 1999 in Nagasaki, Japan. They were followed for incident prostate cancer from July 1958 through December 2004, and the risk of prostate cancer for Brugada-like ECG, age, smoking habit, and radiation exposure was analyzed using Cox proportional hazards analysis. Among the men with or without Brugada-like ECG there were 4 (11.8%) and 54 (2.0%) cases of prostate cancer, respectively. With age adjustment there was a higher risk of prostate cancer for Brugada-like ECG (relative risk (RR): 5.42, 95% confidence interval (CI) 1.96–15.00, P=0.001). With further adjustment for smoking habit and radiation dose, Brugada-like ECG remained a significant risk factor for prostate cancer (RR: 6.47, 95%CI 1.97–21.21, P=0.002).

Conclusions Brugada-like ECG confers a higher risk of prostate cancer independent of age, smoking habit, and radiation exposure. Men with a Brugada-like ECG should be regularly examined for prostate cancer and vice versa, especially elderly subjects. (*Circ J* 2009; **73:** 63–68)

Key Words: Brugada-like ECG; Epidemiology; Prostate cancer

Brugada syndrome (BS) is characterized by a coved-type or type 1 ST-segment elevation in the right precordial leads (V_{1-3}) of the 12-lead electrocardiogram (ECG), as well as symptoms such as documented ventricular fibrillation (VF), polymorphic ventricular tachycardia (VT), family history of sudden death, coved-type ECGs in family members, inducibility of polymorphic VT or VF with programmed electrical stimulation, syncope, or nocturnal agonal respiration[1,2] Several mutations in *SCN5A*, the α subunit of the sodium channel, have been linked to BS[3–5] which displays an autosomal dominant mode of transmission with low penetrance. Although BS is inherited with equal frequency by men and women, most of the reported cases have been in adult men[6,7] In 2 reported cases of Brugada-like ECG, the typical pattern of coved-type ST elevation disappeared following surgical castration for prostate cancer[8] Men with BS have significantly higher plasma testosterone levels than age-matched male controls[9] which suggests that testosterone may contribute to the BS phenotype.

(Received July 15, 2008; revised manuscript received August 21, 2008; accepted August 26, 2008; released online November 29, 2008)

**Department of Cardiovascular Medicine, Course of Medical and Dental Sciences, Graduate School of Biomedical Sciences, Nagasaki University, Departments of **Clinical Studies and †Epidemiology, Radiation Effects Research Foundation, Nagasaki, ††Department of Statistics, Radiation Effects Research Foundation, Hiroshima and ‡Saikakai Shibatachokodo Hospital, Shimabara, Japan*

Mailing address: Daisuke Haruta, MD, Department of Clinical Studies, Radiation Effects Research Foundation, 1-8-6 Nakagawa, Nagasaki 850-0013, Japan. E-mail: harutad@rerf.or.jp

Editorial p35

There is evidence to suggest that testosterone also plays a pathophysiological role in the etiology of prostate cancer. Testosterone is essential for normal growth and maintenance of the prostate, but it also stimulates the proliferation of human prostate cancer cells in vitro and produces prostate cancer in rodents[10,11] Thus, we examined the relationship between the Brugada-like ECG with either the coved-type or saddle-back-type ST elevation and prostate cancer.

Methods

General Procedures

A total of 7,564 atomic bomb survivors (3,374 men; 4,190 women) have been followed biennially in Nagasaki, Japan since July 1, 1958 as part of a follow-up program conducted by the Radiation Effects Research Foundation (RERF). Detailed descriptions of the program have been published elsewhere[12,13] Each examination includes a physical check-up, 12-lead ECG, and blood pressure measurement by sphygmomanometer while the subjects are seated after resting for at least 5 min. First and fifth Korotkoff phases, respectively, are used for the systolic and diastolic blood pressure (SBP and DBP) readings. Standing height (m) and body weight (kg) are measured without socks or outer clothing and the body mass index (BMI: kg/m^2) is calculated. Blood is sampled from a cubital vein for determination of serum cholesterol (mg/dl) and hemoglobin (g/dl). At each examination up to 12 clinical diagnoses are made and stored in a database using the International Classification of Disease (ICD) 7th, 8th, 9th and 10th editions.

Table 1 Number of Subjects With Data Allowing Adjustment for Age Only, Age and Smoking Habit, and Age, Smoking Habit, and Radiation Dose

	Age only	*Age and smoking habit*	*Age, smoking habit, and radiation dose*
Cases with Brugada-like ECG			
With PC	*4 (11.8%)*	*4 (12.5%)*	*3 (16.7%)*
Without PC	*30*	*28*	*15*
Total	*34*	*32*	*18*
Cases without Brugada-like ECG			
With PC	*54 (2.0%)*	*54 (2.2%)*	*36 (2.5%)*
Without PC	*2,593*	*2,379*	*1,400*
Total	*2,647*	*2,433*	*1,436*
Total	*2,681*	*2,465*	*1,454*

ECG, electrocardiogram.

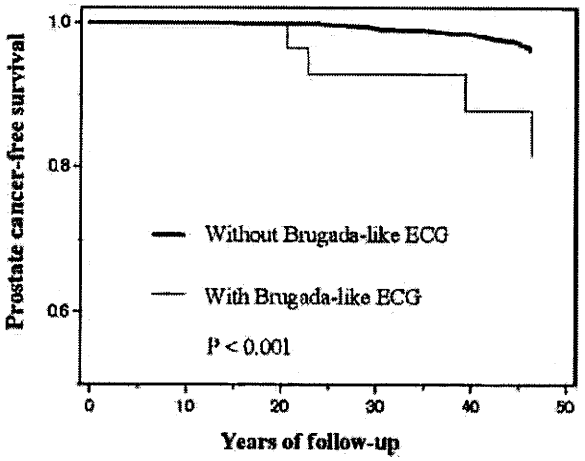

Fig 1. Kaplan-Meier plots showing prostate cancer-free survival, which was lower in cases of Brugada-like electrocardiogram (ECG) than in cases without Brugada-like ECG (P<0.001).

Smoking habit was investigated several times by mail questionnaire and interview during 1963 and 1991; current and past smokers were both regarded as smokers. The present study was approved by the Research Protocol Review and Human Investigation Committees of RERF.

Study Population and Definition of the Brugada-Like ECG

Of the 3,374 men, we investigated 2,681 who had been examined at least once between July 1, 1958 and December 31, 1999. We characterized the ECG as Brugada-like if it showed the following at least once during the follow-up period: (1) terminal r'wave in lead V_1, characterizing right bundle branch block; (2) convex curve or coved-type ST-segment elevation ≥0.1 mV in lead V_1 or in leads V_1 and V_2; or (3) saddle-back-type ST-segment elevation ≥0.1 mV in lead V_2 or V_3, or both. One of the authors (K.M.) made the diagnosis of Brugada-like ECG according to these criteria and this was confirmed by 2 other cardiologists who reviewed the records on which the judgment had been made. We identified 34 cases of Brugada-like ECG, which included 6 cases of unexpected death and 3 cases of syncope, leaving 2,647 men without evidence of Brugada-like ECG. Some aspects of the results were reported previously[6,8,14] Type 1 ST segment elevation characterized by a coved-type ST elevation ≥0.2 mV is included in the diagnostic criteria of BS, whereas Types 2 and 3 ST-segment elevation characterized by a saddle-back ST elevation are not[2] However, to examine the relationship between Brugada-like ECG and prostate cancer, we used wide criteria that included a saddle-back-type ST elevation and elevation ≥0.1 mV.

Confirmation of Prostate Cancer

We identified incident cases of prostate cancer between July 1, 1958 and December 31, 2004 using information from 3 sources. Diagnoses made at biennial health examinations were recorded using ICD codes, as described previously. We followed the vital status of all participants using Japan's family registration system; death certificates were collected for all deceased participants, and prostate cancer as a primary cause of death was recorded according to the coding rules of ICD 7th, 8th, 9th, and 10th editions. The Nagasaki Prefectural Cancer Registry collected and recorded cancer information according to the ICD for Oncology, 1st, 2nd, and 3rd editions. The use of the data of the Nagasaki Prefectural Cancer Registry until 2004 is approved by the Ethics Committee of the Nagasaki Prefectural Cancer Registry. One of the authors (D.H.) reviewed all information from the clinical diagnoses, tumor registry, and death certificates. Prostate cancer cases diagnosed by autopsy only were excluded. In this way 58 cases were ascertained. We defined the date of diagnosis of prostate cancer as follows: (1) in 46 cases of histological examination: the date of histological confirmation; (2) in 12 cases of hormone therapy without histological examination: the date when the clinical diagnosis was made based on digital rectal examination, prostate-specific antigen (PSA) value, and/or bone scintigraphy. Follow-up began in July 1, 1958 and ended on the date of diagnosis of prostate cancer, date of migration or death, or December 31, 2004, whichever came first. Men who died or migrated without a diagnosis of prostate cancer were treated as censored.

Radiation Dose

Because the radiation dose to the prostate is not estimated in the dosimetry system 2002 (DS02),[15] we used the dose to the urinary bladder as a surrogate. The radiation dose in weighted Gray (Gy) equivalents was calculated using a relative biological effectiveness of 10 for neutrons: gamma dose plus 10 times the neutron dose. The gamma and neutron doses were adjusted for 35% random error and truncated at 4 Gy[16,17] to correct for measurement-error bias because of uncertainties in the estimated doses.

Statistical Analyses

At first, Kaplan-Meier analysis was used to assess prostate cancer-free survival between subjects with and without

Table 2 Hazard Ratio (95%CI) of PC for Brugada-Like ECG After Adjustment for Age, Smoking Habit, and Radiation Dose

	Factors adjusted		
	Age only (n=2,681)	*Age and smoking habit (n=2,465)*	*Age, smoking habit, and radiation dose (n=1,454)*
Brugada-like ECG	*5.42 (1.96–15.00) P=0.001*	*5.76 (2.08–15.96) P<0.001*	*6.47 (1.97–21.21) P=0.002*
*Age at start of follow-up**	*2.53 (1.98–3.23) P<0.001*	*2.42 (1.89–3.09) P<0.001*	*2.54 (1.88–3.44) P<0.001*
Smoking habit		*0.55 (0.31–0.97) P=0.04*	*0.56 (0.28–1.13) P=0.11*
Radiation dose (Gy)			*2.12 (1.39–3.22) P<0.001*

**Age was transformed as (age at July 1958–15)/10.*
CI, confidence interval. Other abbreviations see in Table 1.

Table 3 Basic Characteristics at the Most Recent Examination Prior to Diagnosis of PC

	PC with Brugada-like ECG (n=4)	*PC without Brugada-like ECG (n=46)**	*P value*
Age at diagnosis of PC (years)	*72.3±5.8 (n=4)*	*74.2±7.6 (n=46)*	*0.56*
SBP (mmHg)	*144.5±25.2 (n=4)*	*141.0±24.8 (n=45)*	*0.73*
DBP (mmHg)	*78.5±10.4 (n=4)*	*78.6±12.7 (n=45)*	*1.00*
Height (cm)	*160.9±6.9 (n=4)*	*160.2±6.4 (n=41)*	*0.77*
Weight (kg)	*54.5±7.7 (n=4)*	*55.5±9.5 (n=41)*	*0.89*
BMI (kg/m^2)	*20.9±1.3 (n=4)*	*21.6±2.7 (n=41)*	*0.57*
Serum cholesterol (mg/dl)	*184.5±29.7 (n=4)*	*188.2±27.7 (n=44)*	*0.97*
Hemoglobin (g/dl)	*14.6±0.7 (n=4)*	*13.7±1.4 (n=46)*	*0.19*
Smoking habit (%)	*100 (n=4)*	*70.0 (n=46)*	*0.57*
Radiation dose (Gy)	*0.52±0.45 (n=3)*	*0.68±0.64 (n=33)*	*0.82*

Variables are mean±SD.
**Eight cases among the 54 subjects without Brugada-type ECG were excluded because the period between the most recent examination and diagnosis of PC was more than 2 years.*
SBP, systolic blood pressure; DBP, diastolic blood pressure; BMI, body mass index. Other abbreviations see in Table 1.

Brugada-like ECG. Cox regression analysis assuming proportional hazards was used to estimate the prostate cancer incidence rate ratio (relative risk (RR)) and 95% confidence interval (CI) for the Brugada-like ECG. Survival time is the time from inception of the study to the onset of prostate cancer or censoring. Because we cannot check the proportionality assumption for this data because the number of failures is too small, we assumed that the proportional hazard assumption holds for this data. We adjusted for age at the start of follow-up ([age at July 1958–15]/10) using all 2,681 subjects (**Table 1**). Smoking habit was unknown in 216 subjects, resulting in 2,465 subjects for adjustment by both age and smoking habit (**Table 1**). We excluded subjects with unknown dose or who were not in Hiroshima or Nagasaki at the time of the bombing, leaving 1,454 subjects for simultaneous adjustment by age, smoking habit, and radiation dose (**Table 1**).

To assess the basic characteristics of the cases of prostate cancer with Brugada-like ECG, we compared prostate cancer cases with and without Brugada-like ECG using the Wilcoxon rank-sum test or Fisher's exact test, as appropriate, for age at diagnosis of prostate cancer, SBP, DBP, height, BMI, serum cholesterol, and hemoglobin recorded at the last examination prior to diagnosis of prostate cancer, smoking habit, and radiation dose. All analyses were conducted using SAS for UNIX (SAS Institute, Cary, NY, USA).[18] The data are expressed as mean±SD. A P-value less than 0.05 was considered statistically significant.

Results

Prostate cancer occurred in 4 (11.8%) of 34 men with, and 54 (2.0%) of 2,647 men without, Brugada-like ECG (**Table 1**). In the Kaplan-Meier analysis, prostate cancer-free survival was lower in men with the Brugada-like ECG (P<0.001) (**Fig 1**). Hazard ratios with the 3 stages of adjustment (age only; age and smoking habit; and age, smoking habit, and radiation dose) are shown in **Table 2**. Brugada-like ECG was significantly associated with prostate cancer, even after adjustment for age, smoking habit, and radiation dose, although the number of prostate cancer cases among the Brugada-like ECG cases was not so large. There was no interaction of Brugada-like ECG with radiation dose (joint RR: 0.70, 95%CI 0.11–4.38, P=0.70). Smoking habit was negatively associated with prostate cancer in the analysis excluding radiation, but was not significant when radiation dose was included. Radiation dose was a significant risk factor for prostate cancer, even with adjustment for age, smoking, and Brugada-like ECG.

As shown in **Table 3**, there were no differences between the cases of prostate cancer with and without Brugada-like ECG in terms of the variables examined, which suggests that prostate cancer patients do not have clinical or laboratory characteristics that are specific to Brugada-like ECG.

Of the 4 men with prostate cancer and Brugada-like ECG, 2 underwent surgical castration without prostatectomy at ages 67 in 1979 and 78 in 1981, respectively; another under-

Table 4 Age and Date at Diagnosis and Therapeutic Procedure for PC in Cases With or Without Brugada-Like ECG

PC	*Age at diagnosis*	*Date at diagnosis*	*Therapeutic procedure*
With Brugada-like ECG (n=4)			
Case 1	*67*	*1979*	*Surgical castration*
Case 2	*78*	*1981*	*Surgical castration*
Case 3	*68*	*1997*	*Prostatectomy with hormonal castration*
Case 4	*77*	*2004*	*Hormonal castration*
Mean±SD	*72.3±5.8*	*1991±13*	
Without Brugada-like ECG (n=54)	*74.6±7.7*	*1994±9*	*Surgical castration (n=8)* *Prostatectomy with hormonal castration (n=3)* *Hormonal castration (n=22)* *Prostatectomy (n=5)* *Unknown (n=16)*

Abbreviations see in Table 1.

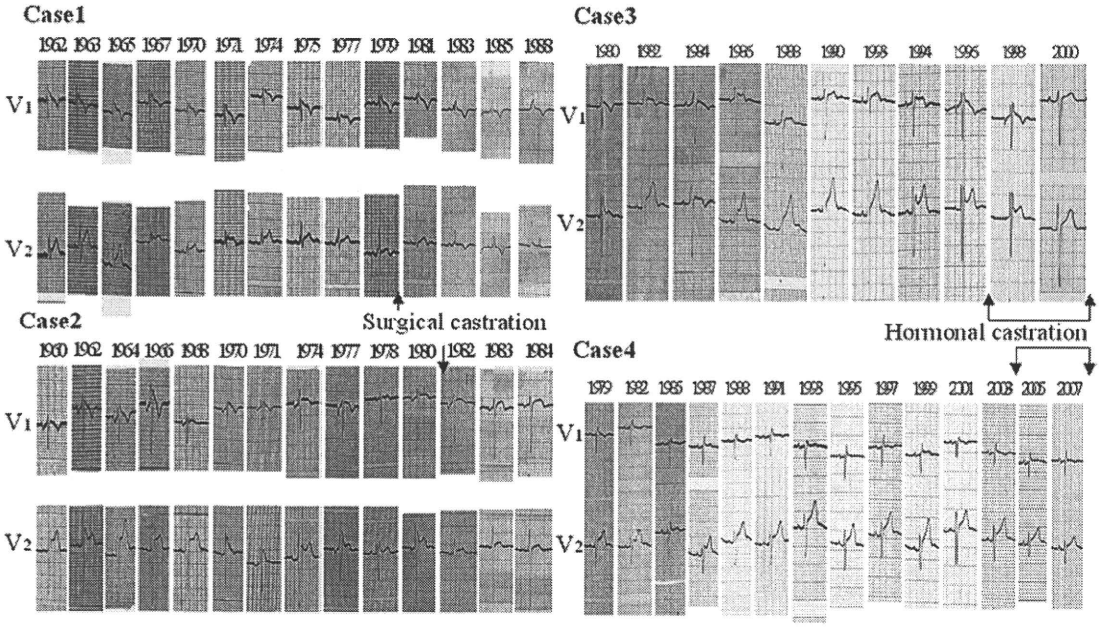

Fig 2. Electrocardiogram (ECG) leads V_1 and V_2. **Case 1**: In 1962, a 49-year-old Japanese man showed the Brugada-like ECG on his 1st examination and it persisted until 1979; the most typical Brugada-like ECG with the coved-type ST elevation in leads V_1 and V_2 was observed in 1971. ST elevation, which was elevated at 0.1 mV in lead V_1 in 1979, disappeared after surgical castration in 1980. He died in 1989 at the age of 76. **Case 2**: In 1960, a 57-year-old Japanese man had his first examination, and in 1962 his ECG showed the Brugada-like ECG, which persisted until 1980, and the most typical Brugada-like ECG with the coved-type ST elevation in leads V_1 and V_2 was observed in 1970. The Brugada-like ECG of the RSr' pattern with the coved-type ST elevation in lead V_1 and the saddle-back-type in lead V_2 disappeared after surgical castration in 1981. He died in 1985 at the age of 82. **Case 3**: In 1979, a 50-year-old Japanese man had his first examination, and in 1980 he had the Brugada-like ECG. The Brugada-like ECG with the coved-type ST elevation in lead V_1 and the saddle-back type ST elevation in lead V_2 was observed in 1996. The Brugada-like ECG gradually disappeared from 1998 to 2000 after the initiation of hormonal castration for prostate cancer in 1997. Because the ECGs in 1990 and 1993 were almost normal, it is possible that this change was just an intermittent normalization. He died in 2001 at the age of 72. **Case 4**: In 1979, a 52-year-old Japanese man had the Brugada-like ECG on his 1st examination. The Brugada-like ECG with the coved-type ST elevation in lead V_1 and the saddle-back-type ST elevation were observed in 1979 and 1985, respectively. In the other ECGs, the Brugada-like ECG has been unclear. He is alive in 2007.

went prostatectomy and hormonal castration with monthly subcutaneous injection of leuprorelin acetate, an LH-RH agonist, and daily oral administration of bicalutamide, an antiandrogen agent since the age of 68 in 1997; and the 4th underwent hormonal castration without prostatectomy, receiving monthly subcutaneous injection of leuprorelin acetate and daily oral administration of bicalutamide since the age of 77 in 2004 (**Table 4**). We have already reported that the Brugada-like ECG pattern with coved-type ST elevation disappeared after surgical castration in cases 1 and 2 (**Fig 2**). In case 3, the Brugada-like ECG pattern disappeared after hormonal castration (**Fig 2**). In case 4, the PSA level decreased from 57.5 (normal range: 1.0–4.0 ng/ml) to an undetectable level (<0.5 ng/ml). However, we could not confirm that disappearance of the Brugada-like ECG pattern was related to hormonal castration because the pattern had been unclear before the initiation of hormonal therapy (**Fig 2**).

Discussion

In the present study, Brugada-like ECG with either coved-type or saddle-back-type ST elevation was significantly associated with prostate cancer risk independently of radiation dose. Thus, this association in male atomic bomb survivors is apparently not mediated through radiation exposure, so the present results may be generalized to men who have not been exposed to radiation.

The association between smoking habit and prostate cancer is equivocal; 1 study reported a positive association,[19] another a negative association[20] and still another no association?[21] Our finding of a positive association between radiation dose and prostate cancer is contrary to 2 previous studies based on atomic bomb survivors?[22,23] In those studies, follow-up beginning in 1958 was continued through 1987 and 1998, respectively, whereas the present follow-up continued through 2004. In recent years, PSA measurement has been widely used for prostate cancer screening, so the relative frequency of prostate cancer diagnosis in the present study (58 prostate cancer cases among 2,681 subjects) was higher than in the study based on follow-up through 1998, which included 387 prostate cancer cases among 42,902 subjects. Greater statistical power resulting from a higher incidence rate may explain in part why we observed an association between radiation dose and prostate cancer.

Recent studies have suggested that the preponderance of males with BS might be attributable to testosterone level. Matsuo et al reported that Brugada-like ECG with coved-type ST elevation disappeared after surgical castration for prostate cancer in 2 cases[8] Shimizu et al reported that men with BS had significantly higher plasma testosterone levels and showed a strong positive association between BS and hypertestosteronemia[9] Yan and Antzelevitch demonstrated that loss of the action potential dome in the epicardium, but not in the endocardium, induced by potassium channel opener causes Brugada-type ECG?[24] By blocking the transient outward potassium current, the epicardial plateau phase is recovered and the ST segment normalizes. Several studies have demonstrated that testosterone increases the outward potassium current or decreases the inward L-type calcium current?[24–27] These reports suggest that high testosterone levels may contribute to the BS phenotype.

There is evidence to suggest that testosterone plays a pathophysiological role in the etiology of prostate cancer. Testosterone is essential for the normal growth and maintenance of the prostate, stimulates the proliferation of human prostate cancer cells in vitro, and when given in large amounts, can produce prostate cancer in rodents![10,11] Eunuchs, on the other hand, rarely develop prostate cancer and ablation of the testosterone-producing cells frequently results in regression of prostate cancer?[28] A high level of circulating testosterone and a low level of sex hormone binding globulin are associated with increased risk of prostate cancer?[29] Dehydrotestosterone (DHT), formed by the action of 5 α-reductase on testosterone, is believed to be the principal intraprostatic androgen, and finasteride, an inhibitor of 5 α-reductase, reduces prostate cancer risk?[30] Testosterone and DHT may be associated with the development of prostate cancer, so we believe that hypertestosteronemia may play a pathophysiological role in both Brugada-like ECG manifestation and prostate cancer, leading to the higher risk of prostate cancer in men with the Brugada-like ECG.

Prostate cancer has been detected more frequently in the early stages of development since the initiation of PSA screening and radical surgical prostatectomy is often performed. Epidural anesthesia using bupivacaine is sometimes used for surgery in early stage prostate cancer and the characteristic coved-type ST elevation is induced by bupivacaine?[31] which causes greater depression of the rapid phase of depolarization in Purkinje fibers and ventricular muscle than lidocaine and remains bound to the sodium channels for a longer period of time?[32] Thus, because we were unable to clarify the clinical and laboratory characteristics of cases of prostate cancer with Brugada-like ECG, it should be carefully ascertained whether the Brugada-like ECG pattern is present before surgery to avoid iatrogenic accidents during epidural anesthesia.

No effective therapeutic strategy exists to prevent VF in BS. An implantable defibrillator is the established therapy to prevent sudden death in symptomatic patients. Among the present cases of Brugada-like ECG pattern with prostate cancer, the Brugada-like ECG disappeared after surgical castration in 2 cases, as reported previously[8] With respect to the 2 hormonal castration cases, we confirmed the disappearance of Brugada-like ECG pattern after hormonal castration in 1 case, but were unable to confirm the effect of hormonal castration on the Brugada-like ECG pattern in another. Because the manifestation of the Brugada-like ECG pattern is associated with testosterone[8,24–27] and BS patients have higher plasma testosterone levels[9] it is important to accumulate more evidence of the Brugada-like ECG pattern disappearing after testosterone deprivation therapy in men with Brugada-like ECG or BS with prostate cancer treated by hormonal castration, which is preferable to surgical castration. This may provide clues to a new therapeutic strategy to prevent VF in BS, although it is necessary to accumulate such evidence in younger cases (40s or 50s in age) of Brugada-like ECG or BS with prostate cancer.

In conclusion, a higher risk of prostate cancer for Brugada-like ECG independent of age, smoking habit, and radiation exposure means that men with the Brugada-like ECG should be regularly examined for prostate cancer, especially elderly subjects. Likewise, prostate cancer patients should be routinely examined for the presence of Brugada-like ECG. Such actions might lead to earlier detection of prostate cancer in a small number of patients, but perhaps more importantly, might avoid arrhythmic events during surgical anesthesia for prostate cancer.

Acknowledgments

The Radiation Effects Research Foundation (RERF), Hiroshima and Nagasaki, Japan is a private, non-profit foundation funded by the Japanese Ministry of Health, Labour and Welfare (MHLW) and the US Department of Energy (DOE), the latter in part through the National Academy of Sciences. This publication was supported by RERF Research Protocol #5–00. The authors thank Ms Kaoru Yoshida and Mr Tomohiro Ikeda for their help in preparation of the manuscript.

References

1. Brugada P, Brugada J. Right bundle branch block, persistent ST segment elevation and sudden cardiac death: A distinct clinical and electrocardiographic syndrome: A multicenter report. *J Am Coll Cardiol* 1992; **20:** 1391–1396.
2. Wilde AA, Antzelevitch C, Borggrefe M, Brugada J, Brugada R, Brugada P, et al. Proposed diagnostic criteria for the Brugada syndrome: Consensus report. *Circulation* 2002; **106:** 2514–2519
3. Chen Q, Kirsch GE, Zhang D, Brugada R, Brugada J, Brugada P, et al. Genetic basis and molecular mechanism for idiopathic ventricular fibrillation. *Nature* 1998; **392:** 293–296.
4. Makita N, Mochizuki N, Tsutsui H. Absence of trafficking defect in R1232W/T1620M, a double SCN5A mutant responsible for Brugada syndrome. *Circ J* 2008; **72:** 1018–1019.

5. Niimura H, Matsunaga A, Kumagai K, Ohwaki K, Ogawa M, Noguchi H, et al. Genetic analysis of Brugada syndrome in Western Japan: Two novel mutations. *Circ J* 2004; **68:** 740–746.
6. Matsuo K, Akahoshi M, Nakashima E, Suyama A, Seto S, Hayano M, et al. The prevalence, incidence and prognostic value of the Brugada-type electrocardiogram, a population-based study of four decades. *J Am Coll Cardiol* 2001; **38:** 765–770.
7. Shimizu W, Aiba T, Kamakura S. Mechanism and new findings in Brugada syndrome. *Circ J* 2007; **71**(Suppl A): A-32–A-39.
8. Matsuo K, Akahoshi M, Seto S, Yano K. Disappearance of the Brugada-type electrocardiogram after surgical castration: A role for testosterone and an explanation for the male preponderance. *Pacing Clin Electrophysiol* 2003; **26:** 1551–1553.
9. Shimizu W, Matsuo K, Kokubo Y, Satomi K, Kurita T, Noda T, et al. Sex hormone and gender difference-role of testosterone on male predominance in Brugada syndrome. *J Cardiovasc Electrophysiol* 2007; **18:** 415–421.
10. Nobel RL. The development of prostate adenocarcinoma in the Nb rat following prolonged sex hormone administration. *Cancer Res* 1977; **37:** 1929–1933.
11. Henderson BE, Ross RK, Pike MC, Casagrande JT. Endogenous hormones as a major factor in human cancer. *Cancer Res* 1982; **42:** 3232–3239.
12. Atomic Bomb Casualty Commission. Research Plan for Joint ABCC-NIH Adult Health Study in Hiroshima and Nagasaki: ABCC Technical Report. Hiroshima and Nagasaki, Japan, 1962; 11–62.
13. Akahoshi M, Soda M, Nakashima E, Shimaoka K, Seto S, Yano K. Effects of menopause on trends of serum cholesterol, blood pressure, and body mass index. *Circulation* 1996; **94:** 61–66.
14. Matsuo K, Akahoshi M, Nakashima E, Seto S, Yano K. Clinical characteristics of subjects with the Brugada-type electrocardiogram: A case control study. *J Cardiovasc Electrophysiol* 2004; **15:** 653–657.
15. Young R, Kerr G, editors. Reassessment of the atomic bomb radiation dosimetry for Hiroshima and Nagasaki, Dosimetry system 2002: Report for the Joint US-Japan Working Group. Hiroshima: Radiation Effects Research Foundation, 2005.
16. Pierce DA, Stram DO, Vaeth M. Allowing for random errors in radiation dose estimates for the atomic bomb survivor data. *Radiat Res* 1990; **123:** 275–284.
17. Preston DL, Pierce DA, Shimizu Y. Effect of recent changes in atomic bomb survivor dosimetry on cancer mortality risk estimates. *Radiat Res* 2004; **162:** 377–389.
18. SAS/STAT software. Changes and Enhancement, Release 9.0. Cary, SAS Institute.
19. Plaskon LA, Penson DF, Vaughan TL, Stanford JL. Cigarette smoking and risk of prostate cancer in middle-aged men. *Cancer Epidemiol Biomarkers Prev* 2003; **12:** 604–609.
20. Veierød MB, Laake P, Thelle DS. Dietary fat intake and risk of prostate cancer: A prospective study of 25708 Norwegian men. *Int J Cancer* 1997; **73:** 634–638.
21. Giovannucci E, Rimm E, Ascherio A, Corditz GA, Spieqelman D, Stampfer MJ, et al. Smoking and risk of total and fatal prostate cancer in United States health professionals. *Cancer Epidemiol Biomarkers Prev* 1999; **8:** 277–282.
22. Thompson DE, Mabuchi K, Ron E, Soda M, Tokunaga M, Ochikubo S, et al. Cancer incidence in atomic bomb survivors. Part II: Solid tumors, 1958–1987. *Radiat Res* 1994; **137**(Suppl): S17–S67.
23. Preston DL, Ron E, Tokuoka S, Funamoto S, Nishi N, Soda M, et al. Solid cancer incidence in atomic bomb survivors: 1958–1998. *Radiat Res* 2007; **168:** 1–64.
24. Yan GX, Antzelevitch C. Cellular basis for the Brugada syndrome and other mechanisms of arrhythmogenesis associated with ST-segment elevation. *Circulation* 1999; **100:** 1660–1666.
25. Shuba YM, Degtiar VE, Osipenko N, Naidenov VG, Woosley RL. Testosterone-mediated modulation of HERG blockage by proarrhythmic agents. *Biochem Pharmacol* 2001; **62:** 41–49.
26. Liu XK, Katchman A, Whitfield BH, Wan G, Janowski EM, Woosley RL, et al. In vivo androgen treatment shortens the QT interval and increases the densities of inward and delayed rectifier potassium current in orchiectomized male rabbits. *Cardiovasc Res* 2003; **57:** 28–36.
27. Bai CX, Kurosawa J, Tamagawa M, Nakaya H, Fukukawa T. Non-transcriptional regulation of cardiac repolarization currents by testosterone. *Circulation* 2005; **112:** 1701–1710.
28. Huggins C, Hodges CV. Studies on prostate cancer: Effect of castration, of estrogen, and of androgen injection on serum phosphatase in metastatic carcinoma of the prostate. *Cancer Res* 1941; **1:** 293–297.
29. Gann PH, Hennekens CH, Ma J, Longcope C, Meir J, Stampfer MJ. Prospective study of sex hormone levels and risk of prostate cancer. *J Natl Cancer Inst* 1996; **88:** 1118–1126.
30. Thompson IM, Goodman PJ, Tangen CM, Lucia MS, Miller GJ, Ford LG, et al. The influence of finasteride on the development of prostate cancer. *N Engl J Med* 2003; **349:** 215–224.
31. Nicole P, Mark P, Robert D, John B. Brugada-type electrocardiographic pattern induced by epidural bupivacaine. *Anesth Analg* 2003; **97:** 264–267.
32. Moller RA, Covino BG. Cardiac electrophysiologic effects of lidocaine and bupivacaine. *Anesth Analg* 1988; **67:** 107–114.

A family of hereditary long QT syndrome caused by Q738X HERG mutation

Shioto Yasuda [a], Shin-ichi Hiramatsu [a], Keita Odashiro [a], Toru Maruyama [a,*], Keiko Tsuji [b], Minoru Horie [b]

[a] The Department of Medicine and Biosystemic Science, Kyushu University Graduate School of Medical Sciences, Fukuoka 812-8582, Japan
[b] Department of Cardiovascular and Respiratory Medicine, Shiga University of Medical Science, Otsu 520-2192, Japan

Received 5 August 2008; accepted 6 December 2008
Available online 21 January 2009

Keywords: Genetic mutation; HERG channel; Long QT syndrome; Torsade de Pointes

Dear Sir,

Hereditary long QT syndromes (LQTS) are autosomal dominant familial disorders characterized by impaired cardiac repolarization and QT prolongation leading to Torsade de Pointes (TdP). Among them, type 2 LQTS (LQT2) is caused by mutations in the human ether a-go-go related gene (HERG) channel gene [1]. Typical ECG manifestation of LQT2 is prolonged QT interval with flat T wave, and TdP is likely to occur at rest by emotional stress evoked by auditory stimuli [2]. Here, we report a small family of hereditary LQT2 caused by a novel HERG mutation, showing a wide variety of ECG phenotypes among family members under the common single nucleotide mutation (c.C2212T and p.Q738X).

A 42-year-old female referred to our hospital due to syncope. ECG showed an increase in QT interval and flat T wave (Fig. 1A). Ambulatory monitoring demonstrated lack of QT shortening under an increase in heart rate during walking. Thereafter, heart rate decreased and QT prolonged further causing short segment of TdP in the morning (Fig. 1B). Although lack of rate adaptation in QT interval was partly restored by propranolol (20 mg/day), she was not tolerant to oral propranolol due to fatigue. Her father underwent pacemaker implantation for back-up pacing against advanced atrioventricular (AV) block, when he was 38-year-old. Thereafter, he exhibited persistent atrial flutter with QT interval of 420 ms at age of 43-year-old (Fig. 1C). Her second daughter is now 10-year-old, and shows long QT interval (480 ms) with broad-based, sharp T wave (Fig. 1D).

Suspecting genetic disorder causing familial LQTS, DNA isolation and mutation analysis were performed as introduced elsewhere [3] after obtaining written informed consent. Gene analysis revealed that the proband, her father and daughter commonly showed a single nucleotide HERG mutation of c.C2212T in a heterozygous manner (Fig. 2) causing a stop codon at 738 (p.Q738X). No other mutations were found in LQTS-associated genes such as KCNQ1, KCNE1, KCNE2, KCNJ2 and SCN5A. By informing of the risk of sudden death, she underwent implantation of dual chamber ICD. After the implantation, she has experienced no syncope without ICD discharge. Her daughter is asymptomatic under careful observation without device or medication.

It is of great interest that ECG phenotypes in this LQT2 family showed a considerable variation, i.e., the proband showed ECG compatible to LQT2 (Fig. 1A) and no rate adaptation of QT interval, postexercise QT prolongation and subsequent TdP (Fig. 1B), which is observed in 13% of overall cardiac events in LQT2 patients [2], whereas her father had advanced AV block and subsequent persistent atrial flutter with normal QT interval (Fig. 1C), and her daughter showed long QT interval with broad-based, tall T wave (Fig. 1D). Reportedly, various kinds of atrial tachyarrhythmias are associated with LQTS [4]. T wave morphology recorded in her daughter is observed mainly in LQT1 but in 32% of LQT2 [3].

HERG K channel conducts rapid component of delayed rectifier K current (I_{Kr}), which is essential for normal cardiac repolarization. To our knowledge, Q738X HERG mutation has not been registered in HERG-related Online Mendelian Inheritance in Man (OMIM; http://pc4.fsm.it:81/cardmoc). The Q738X product results in the deletion of 86% of the C-terminus. Since a single HERG channel protein

* Corresponding author. Tel.: +81 92 642 5235 (direct line); fax: +81 92 642 5247.
E-mail address: maruyama@ihs.kyushu-u.ac.jp (T. Maruyama).

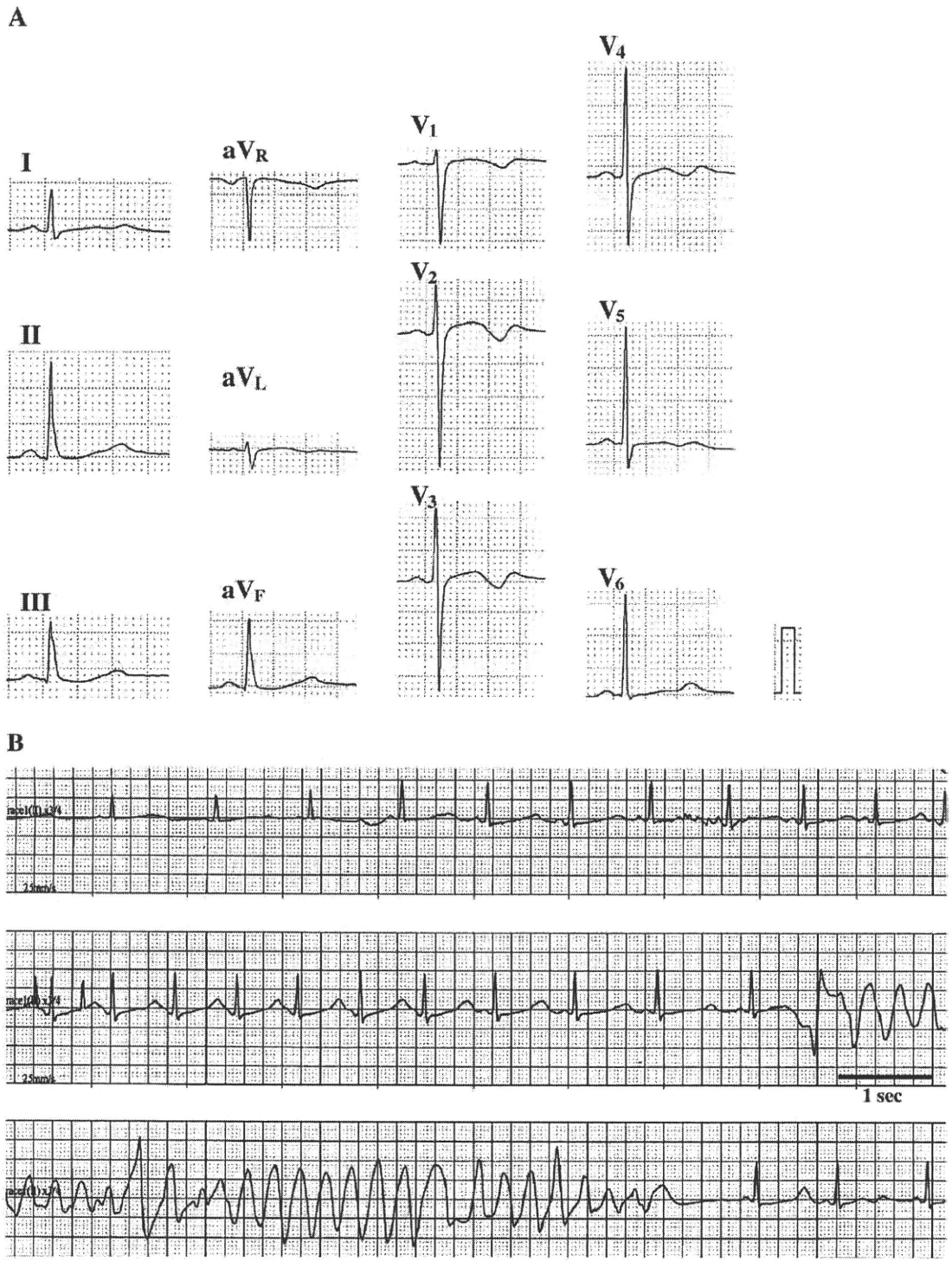

Fig. 1. A; Standard ECG of proband showed QT interval of 520 ms and flat T wave. B; Ambulatory monitoring demonstrated lack of rate adaptation in QT interval and subsequent Torsades de Pointes in the morning. C; Her father showed atrial flutter with ventricular pacing. D; Her daughter exhibited long QT (480 ms) with broad-based, sharp T wave.

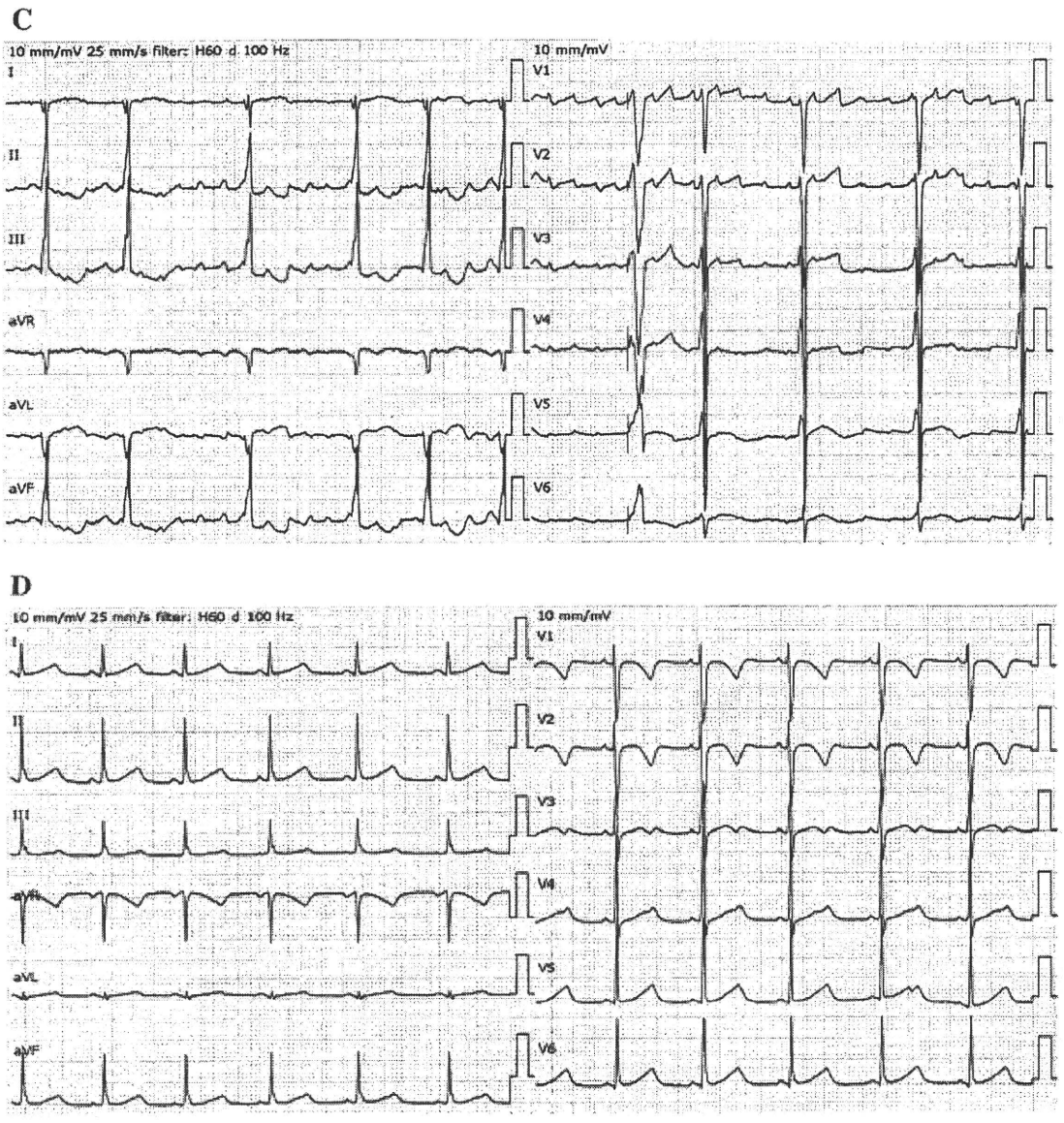

Fig. 1 (*continued*).

consists of four α-subunits, the truncated subunit based on Q738X would hinder the normal assembly of healthy subunits and therefore exerting a dominant negative suppression effects. Although an *in vitro* expression study was not performed, these effects are considered to suppress I_{Kr} profoundly and yield the LQT2 phenotypes in the proband and her family. However, the nonsense Q738X mutation may cause a nonsense-mediated mRNA decay (NMD) and avoid dominant negative suppressions as a post-transcriptional control. The severity of the phenotypes would therefore differ depending on the degree of NMD level [5]. This may be a main reason for varied QT intervals and T wave morphologies in this relatively small LQT2 family.

The authors of this manuscript have certified that they comply with the Principles of Ethical Publishing in the International Journal of Cardiology [6].

References

[1] Curran ME, Splawski I, Timothy KW, Vincent GM, Green ED, Keating MT. A molecular basis for cardiac arrhythmia: HERG mutations cause long QT syndrome. Cell 1995;80:795–803.

[2] Schwartz PJ, Priori SG, Spazzolini C, et al. Genotype–phenotype correlation in the long-QT syndrome. Circulation 2001;103:89–95.

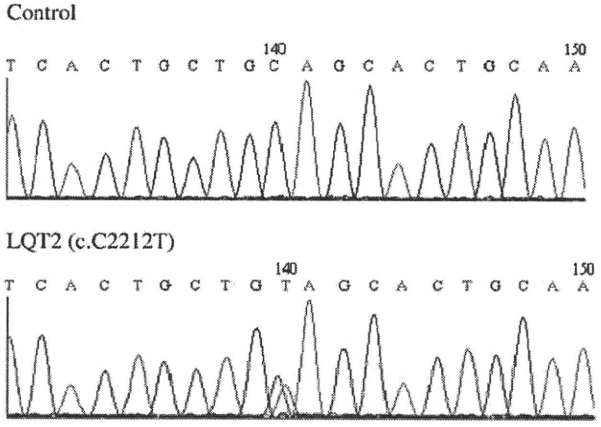

Fig. 2. Mutation analysis of family members. Chromatograms showed a common single nucleotide mutation of c.C2212T, causing amino acid sequence of p.Q738X.

[3] Takenaka K, Ai T, Shimizu W, et al. Exercise stress test amplifies genotype–phenotype correlation in the LOT1 and LQT2 forms of the long-QT syndrome. Circulation 2003;107:838–44.
[4] Kirchhof P, Eckardt L, Franz MR, et al. Prolonged atrial action potential durations and polymorphic atrial tachyarrhythmias in patients with long QT syndrome. J Cardiovasc Electrophysiol 2003;14:1027–33.
[5] Gong Q, Zhang L, Vincent GM, Horne BD, Zhou Z. Nonsense mutations in hERG cause a decrease in mutant mRNA transcripts by nonsense-mediated mRNA decay in human long-QT syndrome. Circulation 2007;116:17–24.
[6] Coats AJ. Ethical authorship and publishing. Int J Cardiol 2009;131: 149–50.

0167-5273/$ - see front matter
doi:10.1016/j.ijcard.2008.12.053

Atrial natriuretic peptide polymorphisms, hydrochlorothiazide and urinary potassium excretion

Stefan Viktor Vormfelde [a,*], Mohammad Reza Toliat [b], Peter Nürnberg [b], Jürgen Brockmöller [a]

[a] *Department of Clinical Pharmacology, University Medical Center, Robert-Koch-Str. 40, 37075 Göttingen, Germany*
[b] *Cologne Center for Genomics (CCG) and Institute for Genetics, University of Cologne, Zuelpicher Straße 47, 50674 Köln, Germany*

Received 6 August 2008; accepted 6 December 2008
Available online 11 January 2009

Keywords: Atrial natriuretic peptide; Genetic polymorphism; Thiazide diuretic; Hydrochlorothiazide; Antihypertensive therapy; Potassium

NPPA disruption goes with salt-sensitive hypertension in mice [1]. In humans, the methionine32 allele of Val32Met (G664A, rs5063) has been associated with low circulating proANP levels [2]. Both methionine32 and the arginine152 allele of the Ter152Arg polymorphism (T2238C, rs5065) have been associated with hypertension or hypertension-related disease (overview in [3]). In conclusion, both variant alleles are supposed to be low functional alleles compared to the respective wild-type alleles. Now, in the ALLHAT study, coronary heart disease outcome tended better or was significantly better in carriers of the variant alleles [3]. In contrast, the overall survival tended lower in these subjects. We explored a potential association of the *NPPA* polymorphisms with diuretic effects of another thiazide diuretic, hydrochlorothiazide, in a single-dose cross-over study with 25 and 100 mg hydrochlorothiazide in 103 healthy, normotensive volunteers.

The study was approved by the Ethics committee of the University of Göttingen; all participants provided written informed consent. The participants were 103 normotensive, healthy, male Caucasian volunteers aged between 18 and

* Corresponding author. Tel.: +49 551 399651; fax: +49 551 12767.
E-mail address: svormfe@gwdg.de (S.V. Vormfelde).

The combination of STFT configuration variables that achieved the highest TDA (86%) was improved in regard to that reported by Barbosa et al. [7]. This indicated that, a larger time window and a larger step between successive time samples best discriminated both groups. Thus, in STFT-derived spectral turbulence analysis, it is possible to consider that the fluctuations of electrical transients are more appropriately defined when analyzing time window is large enough and sample times are apart from each other.

Short and medium term reproducibility studies of spectral turbulence variables have already been carried out elsewhere, to validate present results [8].

In conclusion, spectral resolution affects diagnostic accuracy in SAECG STFT-derived spectral turbulence analysis. An optimal configuration of STFT creation variable combines: 40 ms time window width, 512 points *zero-padding*, 4 ms time displacement steps, −2 ms displacement from starting position. Diagnostic criterion of two abnormal spectral turbulence related variables among four possible, along with STFT configuration that assesses 40 ms time window in the ventricular activation are the optimal configuration allowing for appropriate discrimination between Control and SMVT groups.

The study was supported by Brazilian National Research Council (CNPq).

The authors of this manuscript have certified that they comply with the Principles of Ethical Publishing in the International Journal of Cardiology [9].

References

[1] Ahuja RK, Turitto G, Ibrahim B, Caref EB, El-Sherif N. Combined time-domain and spectral turbulence analysis of the signal-averaged ECG improves its predictive accuracy in postinfarction patients. J Electrocardiol 1994;27(1):202–6.
[2] Vásquez R, Caref EB, Torres F, Reina M, Espina A, El-Sherif N. Improved diagnostic value of combined time and frequency domain analysis of the signal-averaged electrocardiogram after myocardial infarction. JACC 1999;33(2):385–94.
[3] Kelen GJ, Henkin R, Starr A, Caref EB, Bloomfield D, El-Sherif N. Spectral turbulence analysis of the signal-averaged electrocardiogram and its predictive accuracy for inducible sustained monomorphic ventricular tachycardia. Am J Cardiol 1991;67(11):965–75.
[4] Benchimol-Barbosa PR, de Souza Bomfim A, Barbosa EC, et al. Spectral turbulence analysis of the signal-averaged electrocardiogram of the atrial activation as predictor of recurrence of idiopathic and persistent atrial fibrillation. Int J Cardiol 2006;107(3):307–16.
[5] Benchimol-Barbosa PR, Barbosa-Filho J, de Sá CA, Nadal J. Reduction of electromyographic noise in the signal-averaged electrocardiogram by spectral decomposition. IEEE Trans Biomed Eng 2003;50(1):114–7.
[6] Benchimol-Barbosa PR, Muniz RT. Ventricular late potential duration correlates to the time of onset of electrical transients during ventricular activation in subjects post-acute myocardial infarction. Int J Cardiol 2008;129(2):285–7.
[7] Barbosa EC, Benchimol-Barbosa PR, Ginefra P, Albanesi FM. O eletrocardiograma de alta resolução no domínio da frequência. Utilização de correlação espectral para identificação de pacientes com taquicardia ventricular monomórfica sustentada [In portuguese]. Arq Bras Cardiol 1998;71(4):595–9.
[8] Benchimol-Barbosa PR, Bomfim AS, Barbosa EC, Boghossian S, Barbosa-Filho J, Albanesi-Filho FM. Reproducibility of spectral turbulence measurements post ST elevation. Cardiorhythm, 2007, Hong Kong. Europace. Hong Kong: Oxford University Press; 2007. 9:66.
[9] Coats AJ. Ethical authorship and publishing. Int J Cardiol 2009;131:149–50.

0167-5273/$ – see front matter
doi:10.1016/j.ijcard.2009.04.013

A novel SCN5A mutation associated with the linker between III and IV domains of $Na_v1.5$ in a neonate with fatal long QT syndrome

Kenichiro Yamamura [a,*], Jun Muneuchi [a], Kiyoshi Uike [a], Kazuyuki Ikeda [a], Hirosuke Inoue [a], Yasushi Takahata [a], Yuichi Shiokawa [b], Yukako Yoshikane [c], Takeru Makiyama [d], Minoru Horie [e], Toshiro Hara [a]

[a] *Department of Pediatrics, Graduate School of Medical Sciences, Kyushu University, Japan*
[b] *Department of Cardiovascular Surgery, Graduate School of Medical Sciences, Kyushu University, Japan*
[c] *Department of Pediatrics, Fukuoka University Hospital, Japan*
[d] *Department of Cardiovascular Medicine, Graduate School of Medicine, Kyoto University, Japan*
[e] *Department of Cardiovascular and Respiratory Medicine, Shiga University of Medical Science, Japan*

ARTICLE INFO

Article history:
Received 8 April 2009
Accepted 11 April 2009
Available online 6 May 2009

Keywords:
Long QT syndrome
Fetal arrhythmia
SCN5A
Linker of III–IV domains

* Corresponding author. Department of Pediatrics, Graduate School of Medical Sciences, Kyushu University, 3-1-1, Maidashi, Higashi-ku, Fukuoka, 812-8582, Japan. Tel.: +81 92 642 5421; fax: +81 92 642 5435.
E-mail address: yamamura@pediatr.med.kyushu-u.ac.jp (K. Yamamura).

Congenital long QT syndrome (LQTS) is a genetically heterogeneous disorder caused by mutations in cardiac ion channels [1]. Patients with LQTS are predisposed to syncope, life-threatening arrhythmias and sudden death due to delayed ventricular repolarization. Clinical manifestations of LQTS are variable according to gender, age and genetic backgrounds. LQTS concurrent with lower heart rate or atrioventricular block is rare but fatal, which usually manifests itself before birth or during the neonatal period.

The mutation in *SCN5A*, which encodes the alpha subunit of cardiac voltage-gated sodium channel ($Na_v1.5$), is responsible for LQTS type3 (LQT3). As more than 150 mutations in *SCN5A* have been reported [2], several types of mutations such as P1332L and F1473C are associated with intrauterine and neonatal manifestations of LQT3 with the higher mortality [3].

We here present a notable case of a neonate with fatal LQT3 who pre- and postnatally developed atrioventricular block and ventricular tachycardia (VT). Genetic analysis demonstrated a novel *de novo*

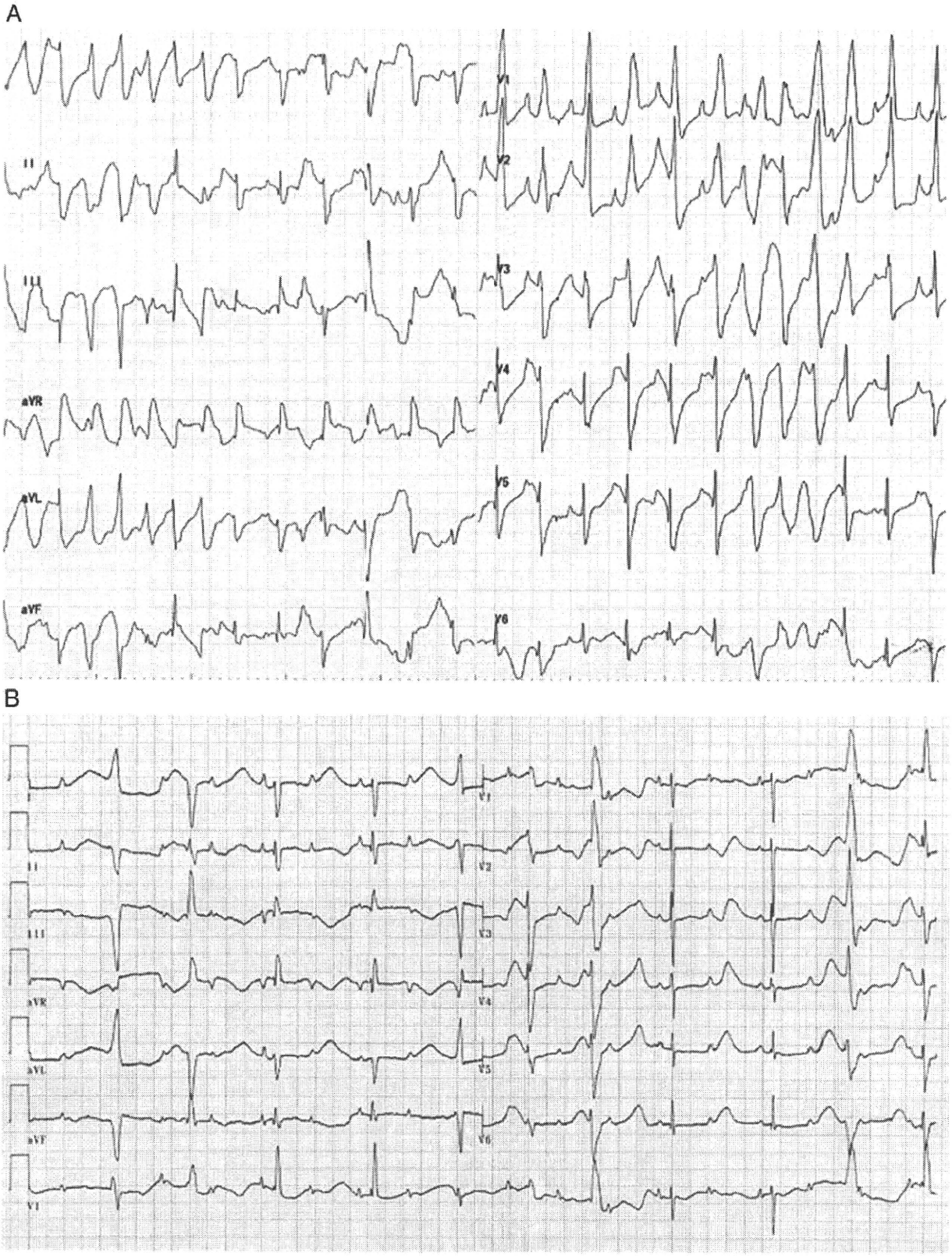

Fig. 1. Twelve-lead electrocardiogram at admission (A), and after administration of amiodarone (B). Paper speed 25 mm/s; 10 mm/1 mV. A, Polymorphic ventricular tachycardia. B, 2:1 Atrioventricular block (HR 56 bpm, atrial rate 112 bpm) due to extremely prolonged corrected QT interval (as long as 860 ms).

heterozygous mutation in SCN5A associated with the linker between III and IV domains of $Na_v1.5$.

A male newborn weighing 2334 g was delivered at 37 weeks of gestation by caesarean section because prenatal ultrasound demonstrated fetal hydrops with atrioventricular block, incessant ventricular tachycardia and decreased ventricular function. There was no maternal obstetrical or medical history. As he had poor perfusion and respiratory insufficiency, assisted ventilation and administration of dobutamine were started. Irregular and weak pulsation was noted. Chest X-ray showed that cardiothoracic ratio was 67%. Echocardiogram showed dilated left ventricle, decreased left ventricular ejection fraction (23%) and significant pericardial effusion. Electrocardiogram (ECG) demonstrated 2:1 atrioventricular block and polymorphic ventricular tachycardia (VT) (Fig. 1A). VT was refractory to intravenous administration of magnesium (50 mg/kg) and lidocaine (3 mg/kg). Although prenatal ultrasound raised the suspicion of LQTS, a definitive diagnosis was not made. To improve the circulatory instability, the patient was given a test dose of intravenous amiodarone (5 mg/kg) which resulted in termination of VT. ECG in sinus rhythm showed 2:1 atrioventricular block (atrial rate of 112 bpm and ventricular rate of 56 bpm) with an excessive QT prolongation (corrected QT interval, 860 ms) and late-appearing T wave (Fig. 1B). However, after a few minutes, ECG demonstrated VT again with following circulatory instability. Further administration of lidocaine, beta-blocker and amiodarone was ineffective. Cardiac pacing was intended to increase heart rate, but in failure. In spite of repetitive cardioversion and chest compressions, he died 18 h after birth. Autopsy was not performed.

There was no family history of prolonged QT interval, syncope, or sudden death. Both parents had screening electrocardiograms with normal QT intervals. There was no sibling.

Genetic DNA was extracted from venous EDTA blood of the present patient and his parents by standard procedure. Because of the ECG phenotype, all coding regions of *SCN5A* were first sequenced directly. Abnormal conformers were amplified by polymerase chain reaction, and sequencing was performed on an ABI PRISM 3100 DNA sequencer (Applied Biosystems, Foster City, California). A heterozygous deletion of TTC at nucleotide position 4456–4458 in exon 26 was detected in the present patient (Fig. 2A). No other mutations were detected in *SCN5A*. We have also found no mutation in *KVLQT1* and *HERG* genes. This nucleotide deletion was predicted to cause an amino deletion of phenylalanine at 1486 (F1486del, III–IV linker of $Na_v1.5$). In a large control population, this mutation was absent, making it less likely that it was a rare polymorphism. Since the mutation was not identified in both parents, we considered it to be a *de novo* mutation.

We present a notable case of a neonate with fatal LQT3 who had a novel *SCN5A* mutation associated with the III–IV linker domain of $Na_v1.5$. In the present case, the corrected QT interval (860 ms) was the longest among the LQTS patients in the previous reports [1,3,4]. To our knowledge, there were only seven case reports of fetal or neonatal onset LQT3 with *SCN5A* mutations [3–9]. A neonate with F1473C mutation in III–IV linker also presented the second longest corrected QT interval (825 ms) which suggested the III–IV linker plays an important role to regulate the sodium channel function [3].

Previous reports indicate that the intracellular loop between domains III and IV of $Na_v1.5$ forms the inactivation gate [10]. A three-residue hydrophobic motif (IFM: 1485I-1486F-1487M) is an essential structural feature of the gate and serves as an inactivation particle that binds within the pore. F1486del mutation identified in the present case resulted in a deletion of the center of this hydrophobic amino acid cluster (Fig. 2B). We considered that F1486del mutation in *SCN5A* is critical to inactivate $Na_v1.5$.

The use of amiodarone was very controversial. ECG after birth was so complicated that we were unable to measure the QT interval exactly. Intravenous amiodarone might have some adverse effects, although it was described that intravenous administration of amiodarone had only little effect to QT intervals [11]. In the present case, the administration of lidocaine was unable to cease VT, although previous reports suggested the efficacy of lidocaine or mexiletine in LQT3 neonates with *SCN5A* mutations. Unfortunately, intravenous mexiletine was not available in our institute. Ruan et al. reported that the response to mexiletine varied among patients harboring different mutations in *SCN5A* [12]. It is assumed that the mutation in III–IV

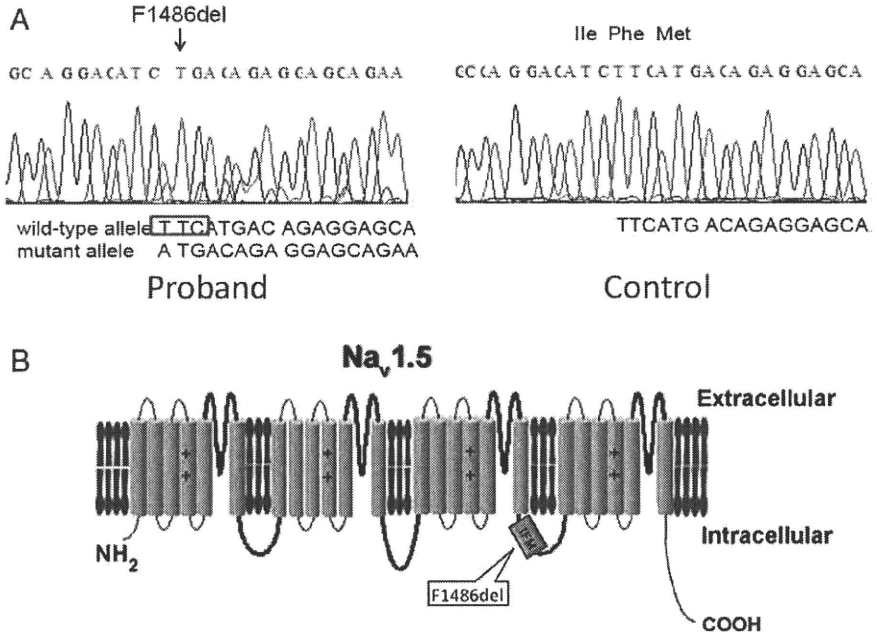

Fig. 2. A, The sequence analysis of exon 26 in *SCN5A*. A heterozygous deletion of TTC at nucleotide position 4456–4458 was detected in the proband. This nucleotide deletion was predicted to cause an amino deletion of phenylalanine at 1486 (F1486del). B, Diagrammatic representation of the human cardiac sodium channel displaying the location of the mutation identified in the present case. F1486del mutation resulted in a deletion of the amino acid in the center of IFM motif.

linker may be associated with the resistance to sodium channel blockers such as lidocaine or mexiletine.

In summary, we identified a novel *de novo SCN5A* mutation in a neonate with extremely prolonged QT interval resulting in cardiac death in the first day of life. This mutation is associated with the IFM motif in the linker between III and IV domains of $Na_v1.5$, which serves as an inactivation particle binding within the pore of sodium channels. This report demonstrates an interesting relationship between clinical phenotype and the location of the mutation and supported the importance of genetic analysis and tailored therapy in neonatal LQTS.

The authors of this manuscript have certified that they comply with the Principles of Ethical Publishing in the International Journal of Cardiology [13].

References

[1] Goldenberg I, Moss AJ. Long QT syndrome. J Am Coll Cardiol Jun 17 2008;51 (24):2291–300.
[2] Remme CA, Wilde AA, Bezzina CR. Cardiac sodium channel overlap syndromes: different faces of SCN5A mutations. Trends Cardiovasc Med Apr 2008;18(3):78–87.
[3] Bankston JR, Yue M, Chung W, et al. A novel and lethal de novo LQT-3 mutation in a newborn with distinct molecular pharmacology and therapeutic response. PLoS ONE 2007;2(12):e1258.
[4] Chang CC, Acharfi S, Wu MH, et al. A novel SCN5A mutation manifests as a malignant form of long QT syndrome with perinatal onset of tachycardia/bradycardia. Cardiovasc Res Nov 1 2004;64(2):268–78.
[5] Wedekind H, Smits JP, Schulze-Bahr E, et al. De novo mutation in the SCN5A gene associated with early onset of sudden infant death. Circulation Sep 4 2001;104 (10):1158–64.
[6] Schulze-Bahr E, Fenge H, Etzrodt D, et al. Long QT syndrome and life threatening arrhythmia in a newborn: molecular diagnosis and treatment response. Heart Jan 2004;90(1):13–6.
[7] Miura M, Yamagishi H, Morikawa Y, Matsuoka R. Congenital long QT syndrome and 2:1 atrioventricular block with a mutation of the SCN5A gene. Pediatr Cardiol Jan–Feb 2003;24(1):70–2.
[8] Ten Harkel AD, Witsenburg M, de Jong PL, Jordaens L, Wijman M, Wilde AA. Efficacy of an implantable cardioverter–defibrillator in a neonate with LQT3 associated arrhythmias. Europace Jan 2005;7(1):77–84.
[9] Miller TE, Estrella E, Myerburg RJ, et al. Recurrent third-trimester fetal loss and maternal mosaicism for long-QT syndrome. Circulation Jun 22 2004;109 (24):3029–34.
[10] McPhee JC, Ragsdale DS, Scheuer T, Catterall WA. A critical role for transmembrane segment IVS6 of the sodium channel alpha subunit in fast inactivation. J Biol Chem May 19 1995;270(20):12025–34.
[11] Kodama I, Kamiya K, Toyama J. Cellular electropharmacology of amiodarone. Cardiovasc Res Jul 1997;35(1):13–29.
[12] Ruan Y, Liu N, Bloise R, Napolitano C, Priori SG. Gating properties of SCN5A mutations and the response to mexiletine in long-QT syndrome type 3 patients. Circulation Sep 4 2007;116(10):1137–44.
[13] Coats AJ. Ethical authorship and publishing. Int J Cardiol 2009;131:149–50.

0167-5273/$ - see front matter
doi:10.1016/j.ijcard.2009.04.023

Predicting prognosis in patients with Chagas disease: Why are the results of various studies so different?

Anis Rassi Jr.*, Anis Rassi

Division of Cardiology, Anis Rassi Hospital, Goiânia, Brazil

ARTICLE INFO

Article history:
Received 14 April 2009
Accepted 23 April 2009
Available online 9 May 2009

Keywords:
Chagas disease
Prognosis
Risk factors
Mortality
Risk stratification
Prediction

The article by Gonçalves and colleagues [1] describes predictors of death among patients with chronic Chagas disease living in an endemic area in Minas Gerais (Brazil). In a retrospective analysis of 120/187 (64.2%) patients with the indeterminate or cardiac form of the disease who could be followed for a mean of 18.5 years, the investigators observed 42 deaths (21 of cardiovascular origin, 7 sudden and 14 due to other causes). Using the Cox regression model, 20 dichotomous demographic, behavioral, clinical and electrocardiographic variables were initially evaluated to calculate the proportional mortality risk from all causes, cardiovascular causes, and sudden death, relative to each variable (univariate analysis). Of these, 12 variables presented statistical significance ($p<0.05$) and were entered into the multivariate model. For all-cause mortality, 5 variables retained independent prognostic significance: age≥39 years (HR 2.19; 95% CI 1.08–4.43; $p=0.028$), black skin colour (HR 6.09; 95% CI 1.23–30.19; $p=0.026$), complete right bundle branch block associated with left anterior fascicular block (HR 34.61; 95% CI 4.32–276.98; $p=0.0008$), complete left bundle branch block (HR 654.92; 95% CI 22.78–18,823.27; $p=0.0002$) and polymorphic ventricular extrasystoles on the 12-lead ECG (HR 8.08 billion; 95% CI 23.76 million to >10E12; $p<0.001$). For cardiovascular mortality, 5 variables were found to be independent prognostic markers in the multivariate analysis: black skin colour (HR 17.72; 95% CI 1.81–172.93; $p=0.013$), complete right bundle branch block associated with left anterior fascicular block (HR 22.86; 95% CI 1.26–413.42; $p=0.034$), complete left bundle branch block (HR 143.73; 95% CI 1.29–15,952.01; $p=0.038$), polymorphic ventricular extrasystoles (HR 921,062.88; 95% CI 234.53–3.62 billion; $p=0.001$) and PR interval ≥0.16 s (HR 9.00; 95% CI 1.98–40.87; $p=0.004$). For sudden death, 4 variables were identified: complete right bundle branch block (HR 233.09; 95% CI 8.57–6339.89; $p=0.001$), left anterior fascicular block (HR 11,490.43; 95% CI 155.24–850,486.33; $p<0.001$), complete left bundle branch block (HR 54,679.94; 95% CI 42.40–70.51 million; $p=0.002$) and polymorphic ventricular extrasystoles (HR 4.04 billion; 95% CI 245,345.20 to >10E12; $p<0.001$).

This investigation reports some unusual findings that merit further discussion. In contrast to other studies, black skin colour, PR interval ≥0.16 s and complete right bundle branch block (amongst others

* Corresponding author. Tel.: +55 62 32279105; fax: +55 62 3227 9311.
E-mail address: arassijr@terra.com.br (A. Rassi Jr.).

Editorial

Bi-directional Ventricular Tachycardia Revised

The nomenclature of bi-directional ventricular tachycardia (BVT) apparently came from its peculiar ECG morphology showing QRS complexes alternatively changing the frontal axis during ventricular tachycardia. Clinically, BVT was reported as early as 1954 and most often seen in digitalis intoxication. The term BVT was therefore not based on the functional mechanism. However, the molecular basis for two types of inherited ion channel diseases that commonly show BVT has recently been partially elucidated. Accordingly, the concept in regard to BVT may require some reconsideration.

Two other pathological conditions with frequently-observed BVT are Andersen-Tawil syndrome (ATS) and catecholaminergic polymorphic ventricular tachycardia (CPVT). **Figure 1** depicts a 12-leads ECG recorded from a case of genotyped ATS. The patient was initially diagnosed with long QT syndrome since her ECG showed a markedly prolonged QT interval and lacked two other clinical hallmarks of ATS: periodic paralysis and dysmorphic features. Cardiac phenotypes in ATS are characterized by prolongation of QT (or QTU) interval associated with various types of ventricular tachycardias including BVT. It is inherited in an autosomal dominant manner and is defined as a potassium channelopathy since it is caused by mutations on the *KCNJ2* gene which encodes for the protein Kir2.1. This potassium channel carries a background K-current (called I_{K1}) whose main feature is to maintain a deep resting membrane potential. *KCNJ2* mutations found in ATS usually produce loss-of-function effects and thus induce a subtle depolarization of the resting membrane potential, which in turn increases the resting intracellular Ca level via the Na/Ca exchanger.

In contrast, mutations in genes encoding for either the ryanodine receptor (RyR2) or the Ca-binding protein (CASQ2) have been shown to cause another type of familial arrhythmia, CPVT. CPVT patients have no structural heart defects and show exercise/emotion-triggered syncope and/or sudden cardiac death mainly during childhood. Inheritance also follows an autosomal dominant trait. Proteins encoded by RyR2 or CASQ2 are both important players for Ca handling of the sarcoplasmic reticulum (SR). In fact, several RyR2 mutations have been shown to increase SR Ca-release into the cytoplasm.

Finally, now coming back to digitalis intoxications, the drug is well known to inhibit membrane Na/K-ATPase and eventually increases intracellular Ca concentration via the Na/Ca exchanger. Therefore, increase in intracellular Ca level turns up to be a common feature among these three distinct diseases. Although a precise mechanism underlying this bizarre form of ventricular tachycardia remains unknown, there may be alternative oscillation in cytosolic Ca concentrations in the presence of severe functional failure of Kir2.1, SR Ca-handling, Na/K-ATPase or Na/Ca exchanger, which may in turn affect the

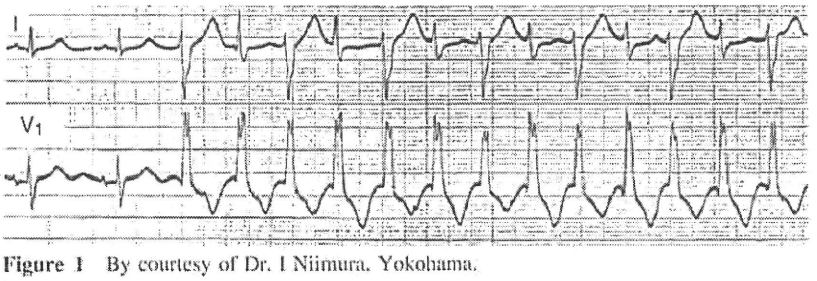

Figure 1 By courtesy of Dr. I Niimura, Yokohama.

morphological ECG features. A computer simulation including intracellular Ca concentrations may offer a clue to answer the mechanistic question in regard to this still-unsolved type of arrhythmia, BVT.

Minoru Horie
Professor,
Department of Cardiovascular Medicine
Shiga University of Medical Science

4

J Membrane Biol (2010) 235:73–87
DOI 10.1007/s00232-010-9257-2

Characterization of the Rapidly Activating Delayed Rectifier Potassium Current, I_{Kr}, in HL-1 Mouse Atrial Myocytes

Futoshi Toyoda · Wei-Guang Ding · Dimitar P. Zankov · Mariko Omatsu-Kanbe · Takahiro Isono · Minoru Horie · Hiroshi Matsuura

Received: 29 November 2009 / Accepted: 29 April 2010 / Published online: 19 May 2010

Abstract HL-1 is the adult murine cardiac cell line that can be passaged repeatedly in vitro without losing differentiated phenotype. The present study was designed to characterize the rapidly activating delayed rectifier potassium current, I_{Kr}, endogenously expressed in HL-1 cells using the whole-cell patch-clamp technique. In the presence of nisoldipine, depolarizing voltage steps applied from a holding potential of −50 mV evoked the time-dependent outward current, followed by slowly decaying outward tail current upon return to the holding potential. The amplitude of the current increased with depolarizations up to 0 mV but then progressively decreased with further depolarizations. The time-dependent outward current as well as the tail current were highly sensitive to block by E-4031 and dofetilide (IC_{50} of 21.1 and 15.1 nM, respectively) and almost totally abolished by micromolar concentrations of each drug, suggesting that most of the outward current in HL-1 cells was attributable to I_{Kr}. The magnitude of I_{Kr} available from HL-1 cells (18.1 ± 1.5 pA pF^{-1}) was sufficient for reliable measurements of various gating parameters. RT-PCR and Western blot analysis revealed the expression of alternatively spliced forms of mouse *ether-a-go-go*-related genes (mERG1), the full-length mERG1a and the N-terminally truncated mERG1b isoforms. Knockdown of mERG1 transcripts with small interfering RNA (siRNA) dramatically reduced I_{Kr} amplitude, confirming the molecular link of mERG1 and I_{Kr} in HL-1 cells. These findings demonstrate that HL-1 cells possess I_{Kr} with properties comparable to those in native cardiac I_{Kr} and provide an experimental model suitable for studies of I_{Kr} channels.

Keywords Cardiac cell line · Potassium current · Potassium channel · Patch-clamp · HL-1 cell · siRNA

F. Toyoda (✉) · W.-G. Ding · D. P. Zankov · M. Omatsu-Kanbe · H. Matsuura
Department of Physiology, Shiga University of Medical Science, Otsu, Shiga 520-2192, Japan
e-mail: toyoda@belle.shiga-med.ac.jp

D. P. Zankov · M. Horie
Department of Cardiovascular and Respiratory Medicine, Shiga University of Medical Science, Otsu, Shiga 520-2192, Japan

T. Isono
Central Research Laboratory, Shiga University of Medical Science, Otsu, Shiga 520-2192, Japan

Introduction

Cardiac delayed rectifier potassium current (I_K) is responsible for action potential repolarization and pacemaker activity and consists of multiple components with distinct time and voltage dependence and pharmacological properties. I_{Kr} is the rapidly activating, inwardly rectifying component of I_K, which can be isolated as a fraction specifically blocked by the class III antiarrhythmic methanesulfonanilide agents such as E-4031 and dofetilide (Sanguinetti and Jurkiewicz 1990). It is now well known that I_{Kr} is conducted by ERG1 (*ether-a-go-go*-related gene) potassium channels (Sanguinetti et al. 1995; Trudeau et al. 1995). Mutations in the human ERG1 (HERG) channel gene underlie the inherited long QT syndrome, a disorder of cardiac repolarization that predisposes affected individuals to life-threatening arrhythmias (Curran et al. 1995). In addition, I_{Kr} is sensitive to block by a diverse range of therapeutic agents (e.g., antihistamines, gastrointestinal prokinetic agents, psychoactive substances), and these adverse drug effects can induce acquired long QT syndrome (Roden et al. 1996).

Taking advantage of molecular biological technology, functional analysis of reconstituted HERG channels in a heterologous expression system has provided information on the gating mechanisms, modulation and drug block of I_{Kr} channels. Nevertheless, current recordings from native channels are still important because several differences between native I_{Kr} and reconstituted HERG current have been revealed (Sanguinetti et al. 1995; Weerapura et al. 2002), possibly due to inadequate composition of channel proteins or lack of cardiac-specific environments in the heterologous expression system. AT-1 cells, a cardiac cell line derived from atrial tumor of adult transgenic mice expressing the simian virus 40 (SV40) large T-antigen targeted to atrial cardiomyocytes via the atrial natriuretic factor (ANF) promoter (Field 1988), have been often employed as a suitable source of native I_{Kr} channels (Liu et al. 1994; Yang and Roden 1996; Yang et al. 1994, 1995, 1997). Membrane current recorded from these cells displays phenotypical characteristics of cardiac I_{Kr} with minimal contamination of other time-dependent outward currents. Maintenance of AT-1 cells, however, is complicated and labored because it is impossible to passage these cells serially in vitro. They are maintained by serial propagation as a subcutaneous tumor in syngeneic mice and have to be used as primary cells (Delcarpio et al. 1991).

The HL-1 cell line was derived from subsequent development of AT-1 cells (Claycomb et al. 1998). Different from any other cardiac cell lines currently available, HL-1 cells can be repeatedly passaged in culture while maintaining a differentiated cardiac phenotype. They express many cardiac-specific proteins such as α-myosin heavy chain, ANF, α-cardiac actin and connexin 43 (Claycomb et al. 1998). Furthermore, several functional receptors, such as α_1-adrenergic and δ-opioid receptors, and intracellular signaling proteins required for phosphatidylinositol hydrolysis and the cyclic AMP synthesis pathway have been demonstrated in HL-1 cells (McWhinney et al. 2000; Neilan et al. 2000; Sartiani et al. 2002). Recent patch-clamp studies have revealed the existence of several cardiac membrane currents, including I_{Kr} as well as the hyperpolarization-activated nonselective cation current (I_f) and the L- and T-type Ca^{2+} currents ($I_{Ca,L}$ and $I_{Ca,T}$) (Claycomb et al. 1998; Sartiani et al. 2002; Xia et al. 2004; Zankov et al. 2009). Thus, HL-1 cells may be used as a model of cardiac cells for studying many features of ion channels in a cardiac-specific environment (White et al. 2004).

The present study characterizes I_{Kr} channels endogenously expressed in HL-1 cells. Whole-cell patch-clamp experiments demonstrate that I_{Kr}, defined as the E-4031-sensitive current, can be elicited in almost all cells with current magnitude of 0.1–1.5 nA suitable for high-quality recording, which allows us to analyze biophysical and pharmacological features extensively and reliably. In addition, alternatively spliced forms of mouse ERG1 (mERG1) are identified in HL-1 cells, and our RNA interference (RNAi) experiments suggest that these ERG1 isoforms indeed underlie I_{Kr}. Data obtained here will be helpful for future applications of HL-1 cells as a unique model to study cardiac I_{Kr} channels.

Methods

Culture of HL-1 Cells

The HL-1 cell culture (passage 36) was a kind gift from Dr. Claycomb (Louisiana State University Health Science Center, New Orleans, LA) who first established the cell line. Care of the HL-1 cells was described previously (Claycomb et al. 1998). Claycomb medium (JRH Bioscience, Lenexa, KS; catalog 51800), a commercially available medium specifically designed for the growth of HL-1 cells, was purchased. Before use, the Claycomb medium was supplemented with 10% fetal bovine serum (JRH Bioscience), 2 mM L-glutamine (Invitrogen, Carlsbad, CA), 0.1 mM norepinephrine (Sigma, St. Louis, MO) and penicillin–streptomycin (Nakalai Tesque, Kyoto, Japan). The supplemented Claycomb medium was prepared every 2 weeks and kept in the dark by covering the medium bottle with aluminum foil because it is highly light-sensitive. Cells were plated on T25 flasks (Techno Plastic Products, Trasadingen, Switzerland; 90025) precoated overnight with 0.00125% fibronectin (Sigma, F1141) in 0.02% gelatin (Difco, Detroit, MI; 0143-17-9) and maintained in supplemented Claycomb medium at 37°C in humidified 5% CO_2 and 95% air. The culture medium was changed daily. After full confluence, cells were dissociated by 0.05% trypsin/EDTA (Invitrogen). Isolated cells were then suspended in Claycomb medium supplemented with 5% fetal bovine serum and antibiotics, and the cell suspension was used for the patch-clamp experiments or split into new flasks for subsequent culturing.

Reverse Transcription-Polymerase Chain Reaction Amplification

HL-1 cells culture (passage 40) and atrial tissue dissected from adult mice were used for mRNA purification. Total RNA from each sample was extracted by the acid guanidium thiocyanate chlorofrom method (Chomczynski and Sacchi 1987). cDNA was synthesized from 5 μg of total RNA with 20 units of RAV-2 reverse transcriptase (Takara, Otsu, Japan) using random primers. PCR for mouse ERG1 isoforms (mERG1a, mERG1a′ and mERG1b) was

performed using the following primer sets reported previously (Clark et al. 2004) (from 5 to 3): ACA CCT TCC TCG ACA CCA TC (sense; position 621–641, accession AF012870) and GCA TCA GGG TTA AGG CTC TG (antisense; position 1405–1424, accession AF012871) for mERG1a, ACC ACT GGC ATA GGA CCA AG (sense; position 839–858, accession AF012870) and the same antisense as for mERG1a for mERG1a′, ATG GCG ATT CCA GCC GGG AA (sense; position 3952–3971, accession AF012871) and GAT GCC ATT GGT GTA GGA CC (antisense; position 8239–8258, accession AF012871) for mERG1b. The reaction included 0.4 µl of cDNA, 2.5 units of KOD dash polymerase (Toyobo, Osaka, Japan), 1 mM KCl, 6 mM $(NH_4)_2SO_4$, 0.1% Triton X-100, 10 µg ml^{-1} BSA, 0.2 mM each of deoxynucleotide triphosphate and 4 pmol primers in 20 ml of 120 mM Tris–HCl buffer (pH 8.0). Amplification was conducted in a thermal cycler using 30 cycles consisting of denaturation at 98°C for 2 s, annealing at 55°C for 2 s and elongation at 72°C for 60 s. PCR products were identified in an ethidium bromide-stained 1.5% agarose gel by electrophoresis.

Western Blotting

HL-1 cells (passages 45–47) were washed with cold phosphate-buffered saline and resuspended in lysis buffer (50 mM Tris–HCl, 5 mM EDTA, 150 mM NaCl, 1% Triton X-100, pH 7.4) supplemented with a mix of protease inhibitors (Complete Mini; Roche, Mannheim, Germany). Cell lysate was centrifuged at 15,000 rpm for 5 min. Total protein was measured using the DC protein assay (Bio-Rad, Richmond, CA). For Western blot assay, 100 µg of total proteins were dissolved in 2 × SDS sample buffer (4% sodium dodecyl sulfate, 125 mM Tris–HCl, 12% 2-mercaptoethanol, 20% glycerol, 0.005% bromophenol blue, pH 6.8) and then sonicated and boiled for 5 min. Samples were resolved on 7.5% SuperSep gel (Wako, Osaka, Japan) and electrotransferred onto a polyvinylidene difluoride (PVDF) membrane (Bio-Rad). The membrane was blocked in Tris-buffered saline (TBS; 10 mM Tris–HCl, 100 mM NaCl, pH 7.5) containing 0.1% Tween-20 and 10% nonfat dry milk for 1.5 h at room temperature and then incubated overnight at 4°C with a rabbit polyclonal anti-ERG1 antibody (Chemicon, Temecula, CA; AB5222) directed against the C terminus (amino acid residues 1121–1137, accession O08962) of rat ERG1, at a dilution 1:200. After washing with TBS-Tween 0.1%, the membrane was incubated with a horseradish peroxidase-conjugated secondary anitibody (Jackson ImmunoResearch, West Grove, PA; 1:5,000) for 1 h at room temperature. Signals were detected using an enhanced chemiluminescence system.

RNAi

Two Stealth small interfering RNA (siRNA) duplex oligonucleotides directed against all transcripts of the mERG1 gene and RNAi-negative control duplex oligonucleotide (ncRNA) were provided by Invitrogen. The siRNA sequences were as follows: siRNA-1, 5′-AGG CUG ACA UCU GCC UAC ACC UGA A-3′; siRNA-2, 5′-UGU CAU UCC GCA GGC GUA CAG ACA A-3′. HL-1 cell culture of nearly confluent (passages 42–45) was transfected with siRNA against mERG1 or nonspecific RNA (ncRNA, 50 pmol), together with a reporter plasmid DNA (pEGFP vector, 0.5 µg) using Lipofectamine 2000 reagent (Invitrogen) according to the manufacture's instructions. Only GFP-positive cells 2 days after transfection were employed for electrophysiological experiments.

Patch-Clamp Recordings

Current recordings from HL-1 cells (passages 38–52) were performed using the whole-cell configuration of the patch-clamp technique (Hamill et al. 1981) with an EPC-8 patch-clamp amplifier (Heka, Lambrecht, Germany). Cells were dissociated from culture dishes by 0.05% trypsin/EDTA, suspended in Claycomb medium and stored at 4°C for a few hours before use. A small aliquot of cell suspension was transferred into a small (0.5 ml) recording chamber placed on the stage of an inverted microscope (TMD-300; Nikon, Tokyo, Japan). After settling to the glass bottom of the chamber (5–10 min), the cells were continuously superfused with normal Tyrode solution (containing appropriate drugs) kept at 25 ± 1°C or 35 ± 1°C, as indicated. Patch-clamp pipettes were prepared from glass capillary tube (Narishige, Tokyo, Japan) on a horizontal pipette puller (P-97; Sutter Instrument, Novato, CA), and the tips were then fire-polished by a microforge (MF-83, Narishige). Pipette resistance was 2–4 MΩ when filled with internal solution. Currents and voltages were digitized and voltage commands were generated through an ITC-16 AD/DA interface (InstruTECH, Long Island, NY) controlled by Pulse/Pulsefit software (version 8.54, Heka).

Data Analysis

Membrane capacitance (C_m) was calculated by fitting a single exponential function to the decay phase of the transient capacitive current in response to ±5-mV voltage steps (20 ms) from a holding potential of −50 mV. The current amplitude was divided by C_m to obtain the current density (pA pF^{-1}). Linear regression analysis was used for correlations. The voltage dependence of current activation and inactivation was determined by fitting the normalized

tail current (I_{tail}) vs. test potential (V) to a Boltzmann function expressed by $I_{tail} = 1/(1 + \exp[(V_{1/2} - V)/k])$ and $I_{tail} = 1/(1 + \exp[(V - V_{1/2})/k])$, respectively, where $V_{1/2}$ is the voltage at which the current is half-activated and k is the slope factor. The time constant for activation (τ_{act}) was determined from a single-exponential fit to the envelop of tail currents obtained after depolarizing pulses for varying durations, and time constants for deactivation (τ_{fast} and τ_{slow}) were obtained by fitting a two-exponential function to the time course of deactivating tail currents. Dose responses for drug block of currents were analyzed by fitting the relative amplitudes of tail currents (y/y_{max}) vs. the drug concentration ([D]) to a Hill function: $y/y_{max} = 1/\{1 + (IC_{50}/[D])^n\}$, where IC_{50} is the half-inhibitory concentration and n is the Hill coefficient. Data were expressed as mean ± SEM. Statistical analysis was performed by means of ANOVA and a post hoc Tukey test.

Solutions and Drugs

Normal Tyrode solution contained (mM) 140 NaCl, 0.33 NaH_2PO_4, 5.4 KCl, 1.8 $CaCl_2$, 0.5 $MgCl_2$, 5.5 glucose and 5 HEPES, pH adjusted to 7.4 with NaOH. The external solution for current recording was made by adding 0.4 μM nisoldipine (as 1 mM stock solution in ethanol) to normal Tyrode solution to eliminate $I_{Ca,L}$. In some experiments, the concentration of KCl was modified to 2 or 10 mM. The internal pipette solution contained (mM) 70 potassium aspartate, 50 KCl, 10 KH_2PO_4, 1 $MgCl_2$, 3 Na_2–ATP, 0.1 Li_2–GTP, 5 EGTA and 5 HEPES, pH adjusted to 7.2 with KOH. Liquid junction potential between the test solution and the pipette solution was measured at around −10 mV and corrected. In order to rule out possible contamination of $I_{Ca,L}$ in our data, all experiments were conducted in the presence of 0.4 μM nisoldipine (a generous gift from Bayer AG, Wuppertal-Elberfeld, Germany), which is specific blocker of $I_{Ca,L}$. E-4031 (Wako), dissolved in distilled water (1 mM) and dofetilide (a generous gift from Pfizer, Sandwich, UK), dissolved in acidified water (pH 4.0, 1 mM), were diluted down to the final concentration in the test solution.

Results

E-4031-Sensitive Current in HL-1 Cells

I_{Kr} was originally identified as a methanesulfonanilide-sensitive component of I_K in guinea pig cardiomyocytes (Sanguinetti and Jurkiewicz 1990). We recorded whole-cell membrane currents from single HL-1 cells before and after application of E-4031 and then analyzed a drug-sensitive current (Fig. 1). Possible participation of other voltage-dependent currents in our data was minimized; i.e., 0.4 μM nisoldipine was included in the bath solution to block $I_{Ca,L}$ (Xia et al. 2004) and membrane potential was held at −50 mV to inactivate $I_{Ca,T}$ (Xia et al. 2004) and avoid I_f activation (Sartiani et al. 2002). Figure 1a shows representative membrane currents in response to 1-s depolarizing (upper panel) and hyperpolarizing (lower panel) pulses to various test potentials, ranging between −80 and +40 mV in 10-mV steps from a holding potential of −50 mV. As shown in the upper panel of Fig. 1a, depolarizing steps activated time-dependent outward currents with amplitudes that increased with depolarization up to 0 mV and then progressively decreased as the potential became more positive (filled circles, Fig. 1d). After return of the membrane to the holding potential, slowly deactivating tail currents were elicited. In contrast, as shown in the lower panel, hyperpolarizing steps induced small-amplitude inward currents with a slight time dependence, which was possibly due to activation of I_f channels, and following depolarizing steps to the holding potential elicited transient inward currents, which may be attributed to activation of $I_{Ca,T}$. When E-4031 (5 μM) was applied to the bath solution, the time-dependent outward current during depolarizing steps as well as the tail current were almost completely abolished, whereas the inward current during the hyperpolarizing pulse was not significantly influenced (Fig. 1b). The currents after exposure to the drug were nearly time-independent and exhibited small conductance with slight outward rectification (open circles in Fig. 1d). E-4031-sensitive currents obtained by digital subtraction of current traces in the presence of drug from those before application of the drug are illustrated in Fig. 1c. The drug-free and the E-4031-sensitive currents showed very similar current–voltage relationships, and both currents have the characteristics of inward rectification at more positive potential than 0 mV, indicating that I_{Kr} is the dominant outward current in HL-1 cells.

The voltage dependence for I_{Kr} activation was determined by measuring the tail amplitude of E-4031-sensitive current. Figure 2a shows the initial part of tail currents elicited upon return of the membrane potential to −50 mV from the 1-s depolarizing steps to test potentials ranging from −40 to +40 mV. The tail current obviously activated at −30 mV and increased in amplitude for the steps up to +10 mV. In Fig. 2b, the amplitude of the tail currents was normalized to the maximum tail current amplitude and plotted as a function of the membrane potential. The $V_{1/2}$ and k, which were determined by curve fitting the data points to a Boltzmann equation, were −20.4 and 8.0 mV, respectively.

In Fig. 3, kinetic properties were determined by measuring time constants for apparent activation and deactivation of I_{Kr}. An envelope-of-tails test was used to assess